INFORMATICA, 2006, Vol. 17, No. 1, 25–38

The Hilbert–Huang Transform for Detection of Otoacoustic Emissions and Time–Frequency Mapping

Artūras JANUŠAUSKAS, Vaidotas MAROZAS,
Arūnas LUKOŠEVIČIUS
Biomedical Engineering Institute, Kaunas Technology University
Studentų 65, 51369 Kaunas, Lithuania
e-mail: artjanu@ktu.lt

Leif SÖRNMO
Signal Processing Group, Lund University
Lund, Sweden

Received: April 2005

Abstract. This paper presents an application of the Hilbert–Huang transform (HHT) and ensemble correlation for detection of the transient evoked otoacoustic emissions (TEOAEs), and high resolution time–frequency mapping. The HHT provides a powerful tool for nonlinear analysis of nonstationary signals such as TEOAEs. Since the HHT itself does not distinguish between signal and noise it was used with ensemble correlation to extract information about intervals with correlated activity. The combination of methods produced good results for both tasks TEOAE detection and time–frequency mapping. The resulting detection performance, using the mean hearing threshold as audiological separation criterion, was a specificity of 81% at a sensitivity of 90% to be compared to 65% with the traditional wave reproducibility detection criterion. High resolution time frequency mapping predicted in more than 70% of the cases hearing loss at a specific frequency in cases of ski-sloping audiograms. The present m ethod does not require a priori information on the signal and may, with minor changes, be successfully applied to analysis of other types of repetitive signals such as evoked potentials.

Key words: otoacoustic emission detection, Hilbert–Huang transform, time–frequency mapping and feature extraction.

1. Introduction

An otoacoustic emission (OAE) is a tiny acoustic signal recorded in the outer ear canal in response to acoustic stimulus. Different studies have shown that OAE can be generated in subjects with hearing levels better than 20–40dB_{HL} (Prieve, 1996; Stenklev and Laukli, 2003; Collet *et al.*, 1991; Bertoli and Probst, 1997). An otoacoustic emission evoked by a short acoustic stimulus is called transient evoked otoacoustic emission (TEOAE). The response of the ear to a transient stimulus is usually recorded 2.5–20 ms post-stimulus.

Transient evoked otoacoustic emissions contain information about a large part of cochlea. The presence of TEOAEs indicate that the preneural cochlear receptor and middle ear mechanisms are able to respond to sound in a normal way (Kemp *et al.*, 1990). Since TEOAEs reflect the cochlea condition, usually absent for a hearing loss of approximately $30dB_{HL}$ or more, they have the potential to be used for objective assessment of hearing function in large populations for screening purposes (Sokol and Hyde, 2002), monitoring influence of noise exposure (Smeatham, 2002) or ototoxic drugs on the hearing system (McFadden and Pasanen, 1994).

Many studies have reported similar results about the time–frequency structure of TEOAE signals: high frequency components are usually located in the part closer to the stimulus, while low frequency components appear later in the signal and last longer (Kemp *et al.*, 1990; Avan *et al.*, 1993; Whitehead *et al.*, 1995). This time–frequency pattern may be explained by the tonotopic frequency analysis of the human cochlea.

Attempts have been made to estimate pure tone hearing thresholds from OAE signal (Waal *et al.*, 2002; Dietl and Weiss, 2004; Gorga *et al.*, 2003). However, the use of TEOAEs for estimation of hearing thresholds is not yet proved in practice because of the large signal variability of similar ears (Robinette, 2003). One reason for the variability is due to excessive noise left after conventional signal processing, e.g., synchronous averaging.

Further improvement of the signal-to-noise ratio (SNR) is possible by exploiting the relative separation between noise and TEOAE signal components in the time–frequency plane. The TEOAE signal is a highly nonstationary, multicomponent signal, whose frequency content varies considerably over time. It has been shown in previous studies that time windowing (Whitehead *et al.*, 1995) and band-pass filtering (Gorga *et al.*, 1993), or, better, both of these techniques (Janušauskas *et al.*, 2001) help to improve the TEOAE signal estimate. These studies use ad hoc defined fixed bandpass filters in order to split the signal in a few frequency ranges, and ad hoc defined time windows for windowing the filtered signal components. These approaches represent a rough estimation of the underlying TEOAE signal location in time frequency plane. We introduced in a recent paper certain adaptivity using the ensemble correlation (EC) technique for defining location and duration of time windows (Janušauskas *et al.*, 2002). As a result, the equivalent time–frequency mask becomes more exact and tailored to the underlying TEOAE signal. However, frequency axis division into fixed octave sub-bands is not adequate to the most probable location of the TEOAE components, and noise, could thus remain in the TEOAE estimate. A recent study went further by introducing adaptivity in the division of the frequency axis (Marozas *et al.*, 2004). The wavelet packet transform was used to adaptively divide the frequency axis into sub-bands. Time windowing of each frequency component was accomplished using a technique similar to the one presented in (Janušauskas *et al.*, 2002). The wavelet packet transform, however, is only semi-adaptive in defining the frequency axis division since it must adhere to a grid defined by the signal sampling frequency and the level of resolution. The fully adaptive frequency axis division into subbands is provided by signal dependent decomposition methods. This makes it possible to precisely extract the location of signal components in the time–frequency plane with

the desired resolution. One such method is the so-called Hilbert–Huang transform (HHT) (Huang *et al.*, 1998), which decomposes the signal into narrow band components. These components are called empirical mode decomposition (EMD) following by calculation of the traditional analytical Hilbert spectrum for each of the extracted components. Finally, the resulting spectra are mapped onto the time–frequency plane with a desirable resolution. The Hilbert–Huang transform has been successfully used in several applications for nonstationary signal analysis (Echavaria *et al.*, 2001; Chau-Huei *et al.*, 2002).

This article has the following structure. In Section 2 we provide a description of the implemented method with a short theoretical background of the Hilbert–Huang decomposition and the ensemble correlation method, being the main components of the proposed TEOAE detection and time–frequency mapping method. The method itself is described in Subsection 2.3. Subsection 2.4 describes the database of TEOAE signals. Results and discussion are found in Sections 3 and 4, respectively.

2. Materials and Methods

2.1. *Empirical Mode Decomposition*

Empirical mode decomposition is a novel method for non-linear and non-stationary data analysis (Huang *et al.*, 1998; Magrin-Chagnolleau and Baraniuk, 1999). This method decomposes the original time series into "monocomponent functions" called intrinsic mode functions, suitable for defining meaningful instantaneous frequency calculation using the Hilbert transform (Huang *et al.*, 1998). An intrinsic mode function (IMF) is, by definition, a function that satisfies two conditions:

- the function should be symmetric in time, and the number of extrema and zero crossings must be equal, or at most differ by one;
- the mean value of the envelope, defined by the local maxima and envelope defined by a local minima must be zero at any function point.

This means that the IMF it is obtained by locally eliminating the superposition of different frequency and amplitude waves, and eliminating signal asymmetries with respect to the zero level. This is done by using the EMD technique, which decomposes the signal into IMFs with an iterative procedure consisting of extrema identification and "sifting" steps, explained below.

Let the original signal $s(t)$ be the input to the sifting process. The signal $s_{i,k}(t)$ defines a component of the sifting process, which for the first iteration is $s_{1,1}(t) = s(t)$. The sifting process consists of the following steps:

1. First, local minima and maxima are extracted from $s_{i,k}(t)$.
2. Lower and upper envelopes are created by interpolation of $s_{i,k}(t)$ between local maxima and minima.
3. The mean value $m_{i,k}(t)$ of the resulting upper and lower envelopes is calculated for each signal point.

4. The resulting $m_{i,k}(t)$ is subtracted from the signal $s_{i,k}(t)$ so that the next component of the sifting process is defined by:

$$s_{i,k+1}(t) = s_{i,k}(t) - m_{i,k}(t). \tag{1}$$

5. The component $s_{i,k+1}(t)$ is checked against the IMF criteria and, if not met, the sifting process (1–4 steps) is repeated with $k = k + 1$.
6. The above steps are repeated until the resulting signal meets IMF criteria and, consequently is IMF $c_i(t)$. To speed up the procedure, a second condition for the signal to be IMF is relaxed when the standard deviation SD, computed from two consecutive sifting is less than 0.2–0.3:

$$SD = \sum_{t=0}^{T} \Big[\frac{|s_{i,k-1}(t) - s_{i,k}(t)|^2}{s_{i,k-1}^2(t)} \Big] < 0.2. \tag{2}$$

The next sifting process starts after subtraction of the extracted IMF $c_i(t)$ from signal $s_{i,k}(t)$, and the resulting signal $r_i(t)$ is input to the successive sifting process:

$$r_i(t) = s_{i,k}(t) - c_i(t), \tag{3}$$

$$s_{i+1,k}(t) = r_i(t), \tag{4}$$

where $k = 1$.

The sifting process is repeated until all, or the required number of IMFs, are extracted from the signal. In the first case the sifting process is terminated when the residual $r_N(t)$ of the sifting process has less than 3 extrema.

The original signal $s(t)$ can be expressed as a sum of extracted IMFs $c_i(t)$ and the residual of the sifting process $r_N(t)$:

$$s(t) = \sum_{i=1}^{N} c_i(t) + r_N(t). \tag{5}$$

Physically, the empirical mode decomposition process can be understood as a step-by-step extraction of the *locally* highest frequency oscillation of the signal progressively forming low-pass intrinsic mode components (Fig. 1).

2.2. *Time–Frequency Signal Representation in Terms of Hilbert Spectrum*

The Hilbert spectrum and the instantaneous frequency is meaningful in the physical sense only when $x(t)$ is a monocomponent ("narrow band" at any time instance) signal (Huang *et al.*, 1998; Kizhner *et al.*, 2004). Intrinsic mode functions satisfy this condition, by calculation of Hilbert amplitudes and instantaneous frequencies for each IMF separately, producing an analytical time–frequency representation of the signal.

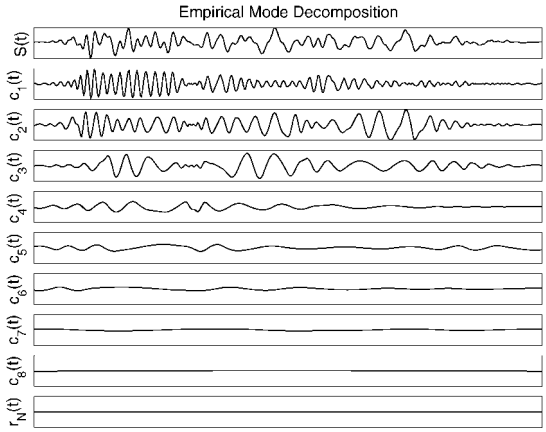

Fig. 1. Signal decomposition into intrinsic mode components.

The signal $s(t)$ may be expressed in terms of analytical amplitudes $A_i(t)$ and instantaneous frequencies $w_i(t)$ (Huang *et al.*, 1998; Kizhner *et al.*, 2004):

$$s(t) = Real\Big\{\Sigma_{i=1}^{N} A_i(t)\mathrm{e}^{j\int w_i(t)\,\mathrm{d}t}\Big\}, \tag{6}$$

$$w_i(t) = \frac{\mathrm{d}\theta_i(t)}{\mathrm{d}t}, \tag{7}$$

where $A_i(t)$ and $\theta_i(t)$ denote the Hilbert transform modulus and phase, respectively, obtained by applying the Hilbert transform on the IMF $c_i(t)$.

A time–frequency signal representation, or a nominal Hilbert spectrum, is constructed by aggregating instantaneous frequencies and corresponding amplitudes of IMFs into defined frequency bins, displayed in a three dimensional time, frequency and Hilbert amplitude space. The Hilbert amplitude represent the square root of the local signal energy. Another representation of Hilbert spectrum is the two dimensional view called marginal Hilbert spectrum, obtained by summing up the amplitudes along the frequency bin time lines and displaying it in amplitude–frequency plane.

2.3. *Algorithm of the Method*

The present method for detection of otoacoustic emission and time–frequency mapping consists of two main branches related to detection and visualization of the signal, see Fig. 2.

Detection is based on weighting of OAE signal sub-averages by ensemble correlation (EC) function and successive cross-correlation decision parameter calculation. The ensemble correlation function itself is a one-weight filter which weights each sample of the averaged signal in relation to the correlation across ensemble of signal realizations (Atarius and Sörnmo, 1995; Janušauskas *et al.*, 2002). Information contained in the EC function allows analysis of signal time intervals with a high SNR.

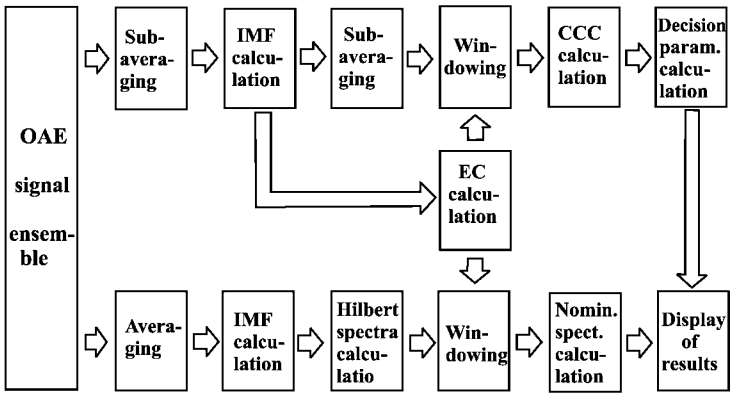

Fig. 2. Block diagram of the method.

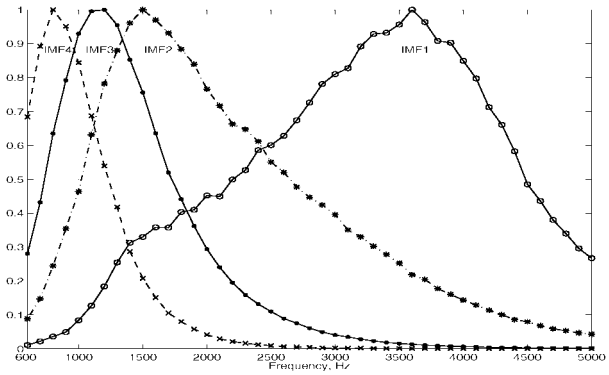

Fig. 3. Normalized averages of the marginal Hilbert spectra of 1000 normal hearing subjects for first four intrinsic mode components.

The first step in OAE detection is to enhance the SNR by sub-averaging the raw TEOAE ensemble into N averages consisting of non-overlapping responses. The number of sub-averages should be chosen large enough for EC function calculation, while small enough for reaching acceptable SNR in each subaverage. In the present method the number of sub-averages was set to 12.

Each subaverage was decomposed into IMFs (Fig. 2), having have variable, signal dependent spectral content. Experiments, however, showed that the frequency range of interest (0.6–6 kHz) is mostly covered by the first four IMFs (Fig. 3). Thus, only these four were used for further computations.

According to the algorithm, the corresponding IMFs were averaged into two non-overlapping sub-averages for each of the 4 IMFs. Signal regions weighted by EC values larger than 0.6, as calculated for each set of components, were used for crosscorrelation coefficient calculation. A restriction of 2 ms minimum length of the overall correlated activity was added to avoid short term correlated noise. In the case when correlated activity was shorter than 2 ms, crosscorrelation coefficient without using EC function weighting

was calculated.

Different detection parameters were investigated and the most successful ones were chosen for further investigation:

1) an average of the four crosscorrelation coefficients as calculated from IMFs 1–4 subaverages, labeled *ccc14*;
2) an average of three crosscorrelation coefficients as calculated from IMFs 1–3 subaverages, labeled *ccc13*;
3) combined detection parameter: TEOAE was detected when at least two crosscorrelation coefficients, as calculated from IMFs 1–3 subaverages, exceeded criterion value, labeled *pass13*;
4) Wave reproducibility is used in the ILO (Otodynamic Inc) commercial TEOAE recording and analysis equipment, and is calculated as the crosscorrelation coefficient between two subaverges, labeled *cccilo*.

Estimation of the time–frequency OAE spectrum is based on the calculation of instantaneous frequencies for the first four IMFs using the Hilbert transform, with the following formation of time–frequency spectra, and displaying only high SNR spectral components.

First, all TEOAE signal realizations from the chosen record were averaged for SNR enhancement. The averaged signal was then decomposed into four IMFs (Fig. 2). Next, the Hilbert analytical amplitudes and instantaneous frequencies were calculated for these components. The nominal Hilbert spectrum was formed by aggregating instantaneous frequencies and corresponding amplitudes into 100 Hz frequency bins. Signal parts from the time regions weighted by ensemble correlation function values lower than 0.6 were excluded from the spectra. A contour plot of amplitudes higher than 0.15 from the maximum amplitude level was presented.

2.4. *Database*

A database with raw TEOAE signals was used for evaluation of the present method, consisting of more than 10000 TEOAE records from adult subjects recorded in an attenuation booth or in a relatively quiet room (Engdahl, 2002; Engdahl and Tambs, 2002). The database contains TEOAE signals from adults with an average age of 49 years (standard deviation 16 years) ranging from 20 to 96 years. All signals were linked to audiograms and other audiological data. The average mean hearing level of the subjects was $16 dB_{HL}$ (standard deviation $15 dB_{HL}$) ranging from -10 to $114 dB_{HL}$.

Signals were recorded by the ILO92 commercial equipment and stored before software processing. Each TEOAE signal ensemble consisted of every response to a four click stimulus train prior to averaging and filtering. Every signal was bandlimited to 600Hz–6kHz and windowed between 2.5–20 ms post-stimulus time.

For the method evaluation the database of TEOAE responses were divided into “normal hearing” (NH) and “hearing impaired” (HI) groups. An audiological separation criterion for NH and HI subjects was set to a mean hearing level of $30 dB_{HL}$ calculated from hearing thresholds at 500Hz, 1kHz, 2kHz and 4kHz. Such a separation resulted in 4228 subjects classified as normal hearing and 761 as hearing impaired. It was assumed that NH subjects should have TEOAE while HI should not.

Approximately 50% of the database, with TEOAEs recorded from the right ears, were used for method development, while the other 50% (left ear records) was used for calculation of results.

To investigate possibility of the method to predict hearing loss at a specific frequency, the "sloping hearing loss" group was formed of 400 TEOAE responses from subjects with sloping hearing loss (hearing level better than $20dB_{HL}$ at 1kHz and worse than $35dB_{HL}$ at 4kHz).

3. Results

The present method was applied to the TEOAE database for objective separation of "normal hearing" (NH) and "hearing impaired" (HI) subjects, as described above. Receiver operating characteristics were calculated for different detection criteria (Fig. 4), as specified in Section 2.3.

At a detection specificity of 90%, "*ccc14*" decision parameter, which uses four first IMFs, gave the best results in terms of sensitivity, however, "*ccc13*" and "*pass13*" that uses the three first IMFs gave similar performance (Table 1). All the decision parameters performed significantly better than did the traditional "*cccilo*" decision parameter.

The possibility to predict hearing loss at a specific frequency was also investigated using signals from subjects with sloping hearing loss as described in Section 2.4. In a

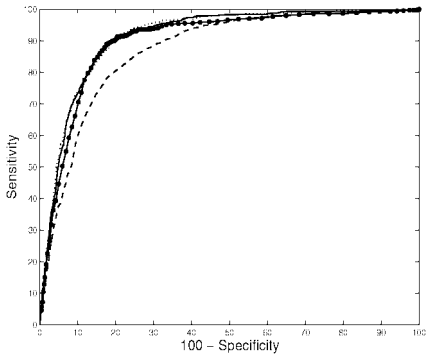

Fig. 4. Receiver operating characteristics for different TEOAE detection criteria: $ccc13$ (solid line), $ccc14$ (dotted), $cccilo$ (dashed) and $pass13$ (solid dotted).

Table 1

TEOAE detection results

Decision parameter	Specificity at 90% sensitivity
ccc13	79.97
ccc14	80.88
pass13	80.42
cccilo	65.43

number of cases it was found that OAE signal time–frequency distribution can predict high frequency hearing loss; this could be observed both in individual cases and in average (Fig. 5). The receiver operating characteristic was calculated for *ccc1* detection parameter, the crosscorrelation coefficient of the first IMF component sub-averages, versus the hearing level at 4kHz.

In this case prediction was lower than overall mean hearing level prediction of the method. The sensitivity at 90% specificity was 70.09% to be compared with 80.88% when detecting mean hearing level using *ccc14* (see Fig. 5).

The same results could be observed in individual signal cases as well. Usually the Hilbert spectrum corresponded quite well to subject's audiogram. Normal hearing subjects had a richer spectral content than had subjects with sloping hearing loss (Figs. 6 and 7). In Fig. 6, OAE spectrum had strong high frequency components up to 6 ms post stimulus time while components in the frequency range 600Hz–2kHz were present throughout the recording. In Fig. 7, the subject with a high frequency hearing loss exhib-

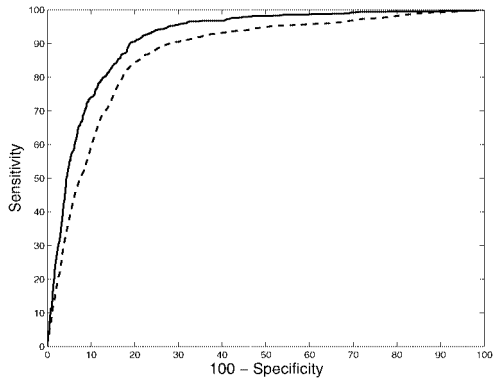

Fig. 5. Receiver operating characteristic showing the capability to predict high frequency hearing loss, using $ccc1$ (dashed line). The ROC for overall TEOAE detection criterion $ccc14$ (solid line) is given for the comparison.

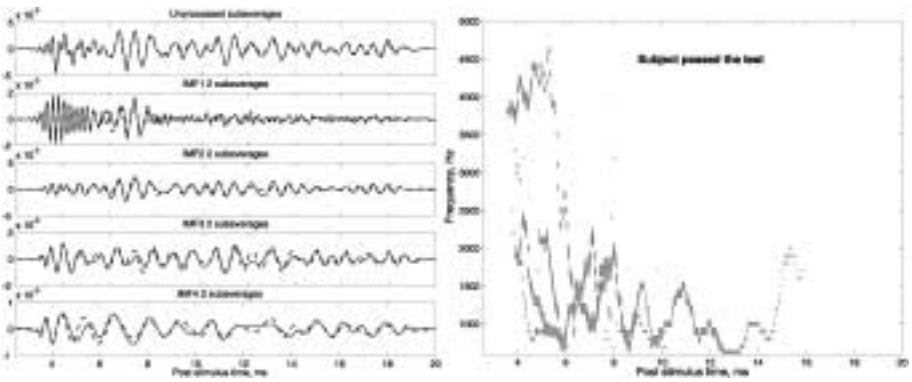

Fig. 6. TEOAE IMFs (two sub-averages) and nominal Hilbert spectrum from a normal hearing subject.

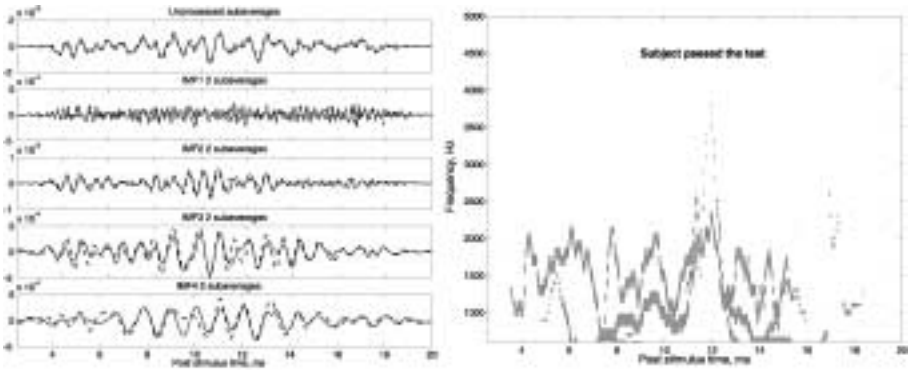

Fig. 7. TEOAE IMFs (two sub-averages) and nominal Hilbert spectrum from a subject with sloping hearing loss.

ited almost no OAE high frequency components extracted by the present method, while the lower frequencies were present throughout the recording. This corresponds to the subject's audiogram with hearing levels better than $30dB_{HL}$ at frequencies up to 2kHz, and worse than $35dB_{HL}$ at higher frequencies.

The results from hearing impaired subjects were not shown since they usually exhibited a very narrow time–frequency range, or no signal components were detected because of low ensemble correlation.

4. Discussion and Conclusions

The introduced method provided us with an accurate equivalent time–frequency mask, to regain the TEOAE signal from noise, and resulted in high TEOAE signal detection performance on a database of almost 5000 TEOAE signals. The HHT-based high resolution time–frequency distributions of TEOAE signals revealed fine time–frequency properties of these signals.

Our implementation of the HHT differs slightly from the original one presented by N. Huang (Huang *et al.*, 1998). Usually cubic spline interpolation technique is used in the EMD, however, it was found that piecewise cubic Hermite interpolation is more suitable for this application. Empirical mode decomposition using Hermite polynomials resulted in more IMFs, but the IMFs had more reiterate frequency content when compared to spline interpolation technique (Kizhner *et al.*, 2004). The frequency resolution of nominal Hilbert spectra was set to 100Hz, and only normalized signal components that exceeded a level of 0.15 were included in the spectra. Such an artificial amplitude and frequency resolution reduction was found to be useful for investigation of signal trends. The use of a higher resolution would result in masking of general trends by accidentally picking noise or tiny signal ripple.

The HHT was found able to extract signal specific time–frequency features. Signals recorded from normal hearing subjects usually had a typical "boomerang" shape time–frequency distribution (Fig. 8), while subjects with high frequency hearing loss had flattened spectra (Fig. 9).

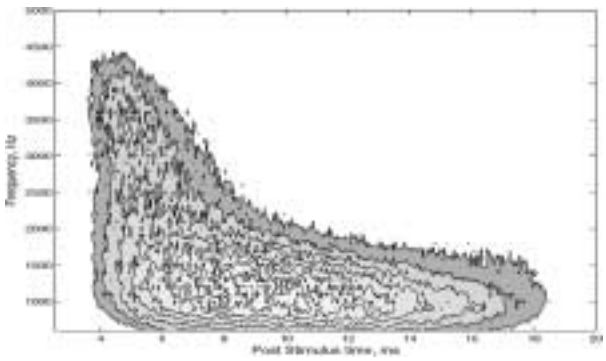

Fig. 8. Average of nominal Hilbert spectra of 1500 good quality normal hearing subjects. Contour plot.

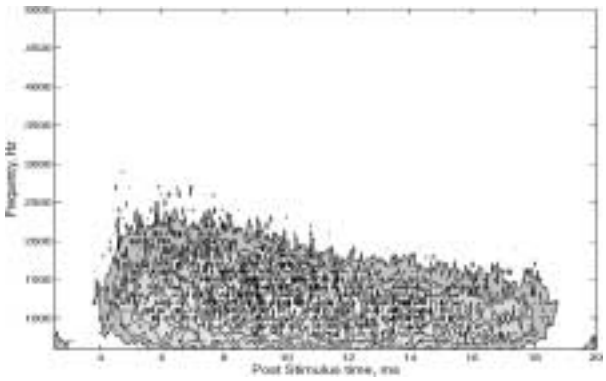

Fig. 9. Average of nominal Hilbert spectra of 400 subjects with sloping high frequency hearing loss. Contour plot.

The present method was found useful for TEOAE signal detection. All decision parameters resulted in higher detection rates than did the traditional crosscorrelation coefficient as used, e.g., in commercial ILO OAE recording and analysis equipment. A number of other decision parameters were investigated during the present study. The use of other IMF combinations or parameters that included signal energy, however, provided worse results. The preference to use decision parameters that do not take energy into account is confirmed by another study (Marozas *et al.*, 2004). The use of only the first four IMFs could be explained by the fact that the TEOAE signal was filtered between 600Hz and 6kHz and the audiological criterion, mean hearing threshold, was traditionally calculated as an average of pure tone hearing thresholds at 0.5kHz–4kHz. It was shown that, in average, the first four IMFs cover this frequency range (Fig. 3) and higher IMFs rapidly decreases in amplitude (Fig. 1) adding no significant information.

A high detection rate (Figs. 4,5, Table 1) and a capability to extract time–frequency features corresponding to other audiological data (Figs. 6–10) suggest that method is able to extract true TEOAE signal features from the recorded signal.

Methods using a priori knowledge about TEOAE latency properties may have higher

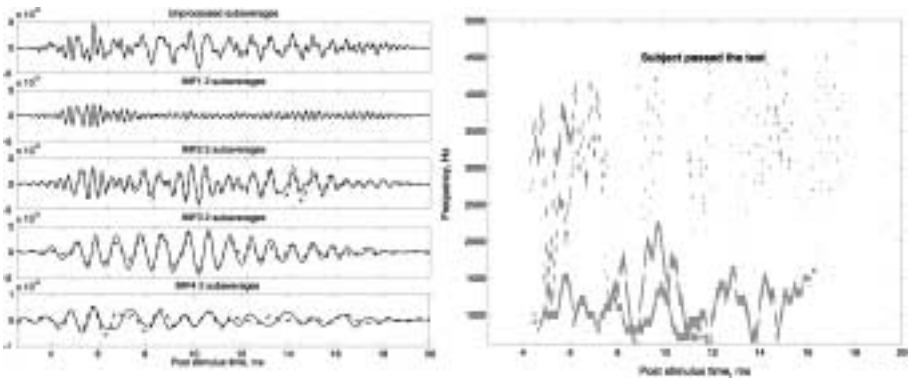

Fig. 10. TEOAE IMFs (two sub-averages) and nominal Hilbert spectrum from normal hearing subject. High frequency OAE present throughout all the signal duration.

detection quality (Janušauskas *et al.*, 2001; Janušauskas *et al.*, 2002). The most important result of this study is, however, the correct estimation of very subtle time–frequency features of an individual TEOAE signal while the detection part of the method, which uses the same principles as time–frequency mapping part proves reliability of the results.

The fact that the present method does not use a priori knowledge on signal properties is an advantage which makes it versatile and directly applicable to both children and adult TEOAE data with quite different latency patterns. For the same reasons the method is easily applicable to other types of repetitive signals, e.g., evoked potentials.

The method was found useful for both detection and investigation purposes. As described above, the TEOAE frequency content can sometimes predict high frequency hearing loss (Fig. 7). The signal pattern itself may vary considerably from subject to subject (compare Figs. 6 and 10). Extraction of tiny signal features could be useful for TEOAE phenomenon investigation, modeling and extracting of the new OAE signal and OAE phenomenon features.

In its current form, the method is only suitable for off-line analysis, since it is time consuming and requires significant computational power. The development of a hardware-based HHT calculation equipment may, however, remove this drawback and widen its application area (Kizhner *et al.*, 2004).

References

Atarius, R., and L. Sörnmo (1995). Signal-to-noise ratio enhancement of cardiac late potentials using ensemble correlation. *IEEE Trans. Biomed. Eng.*, **42**(11), 1132–1137.

Avan, P., P. Bonfils, D. Loth and H.P. Wit (1993). Temporal patterns of transient-evoked otoacoustic emissions in normal and impaired cochleae. *Hear. Res.*, **70**, 109–120.

Bertoli, S., and R. Probst (1997). The role of transient otoacoustic emission testing in evaluation of elderly persons. *Ear Hear*, **18**(4), 286–293.

Chau-Huei, C., L. Cheng-Ping and T. Ta-Liang (2002). Surface-wave dispersion measurements using Hilbert–Huang transform. *TAO 2002*, **13**(2), 171–184.

Collet, L., E. Veuillet, J.M. Chanal and A. Morgon (1991). Evoked otoacoustic emissions: correlates between spectrum analysis and audiogram. *Audiology*, **30**, 164–172.

Dietl, H., and S. Weiss (2004). Detection of cochlear hearing loss applying wavelet packets and support vector machines. In *Proc. of 38th Asilomar. Conf. on Signals, Systems, and Computers*, Pacific Grove, CA. pp. 1575–1579.

Echeveria, J.C., J.A. Crowe, M.S. Woolfson and B.R. Hayes–Gill (2001). Application of empirical mode decomposition to heart rate variability analysis. *Med. Biol. Eng. Comput.*, **39**, 471–479.

Engdahl, B. (2002). Otoacoustic emissions in the general adult population of Nord-Trøndelag, Norway: I. Distributions by age, gender, and ear side. *Int. J. Audiol.*, **41**(1), 64–77.

Engdahl, B., and K. Tambs (2002). Otoacoustic emissions in the general adult population of Nord-Trøndelag, Norway: II. Effects of noise, head injuries, and ear infections. *Int. J. Audiol.*, **41**(1), 78–87.

Janušauskas, A., V. Marozas, B. Engdahl, H.J. Hoffman, O. Svensson and L. Sörnmo (2001). Otoacoustic emissions and improved pass/fall separation using wavelet analysis and time windowing. *Med. Biol. Eng. Comput.*, **39**, 134–139.

Janušauskas, A., L. Sörnmo, O. Svensson and B. Engdahl (2002). Detection of transient evoked otoacoustics emissions and design of time windows. *IEEE Trans. Biomed. Eng.*, **49**(2), 132–139.

Gorga, M.P., S.T. Neely, B.M. Bergman, K.L. Beauchaine, J.R. Kaminski, J. Peters, L. Schulta and W. Jesteadt (1993). A comparison of transient-evoked and distortion product otoacoustic emissions in normal-hearing and hearing-impaired subjects. *J. Acoust. Soc. Am.*, **94**, 2639–2648.

Gorga, M.P., S.T. Neely, P.A. Dorn and B.M. Hoover (2003). Further efforts to predict pure-tone thresholds from distortion product otoacoustic emission input/output functions. *J. Acoust. Soc. Am.*, **113**(6), 3275–3284.

Huang, N., Z. Shen, S. Long, M. Wu, H. Shih, Q. Zheng, N. Yen, C. Tung and H. Liu (1998). The empirical mode decomposition and Hilbert spectrum for nonlinear and non-stationary time series analysis. In *Proc. R. Soc. London*, Vol. 454. pp. 903–995.

Kemp, D.T., S. Ryan and P. Bray (1990). A guide to the effective use of otoacoutic emissions. *Ear Hear*, **11**(2), 93–105.

Kizhner, S., P. Flatley, E.N. Huang, K. Blank and E. Conwell (2004). On the Hilbert–Huang transform data processing system development. In *Proc. IEEE Aerospace Conf.*, Vol. 3. pp. 1961–1979.

Magrin–Chagnolleau, I., and R.G. Baraniuk (1999). Empirical mode decomposition based time–frequency attributes. In *Proc. 69th SEG Meeting*. Houston, US.

Marozas, V., L. Sörnmo, A. Janušauskas and A. Lukoševičius (2004). Multiscale detection of transiently evoked otoacoustic emissions. In *Proc. 6th Nordic Signal Proc Symp NORSIG 2004*, Espoo, Finland. pp. 184–187.

McFadden, D., and G.E. Pasanen (1994). Otoacoustic emissions and quinine sulphate. *J. Acoust. Soc. Am.*, **99**(5), 3460–3474.

Prieve, B.A. (1996). Click and tone-burst-evoked otoacoustic emissions in normal and hearing impaired ears. *J. Acoust. Soc. Am.*, **99**(5), 3077–3086.

Robinette, M.S. (2003). Cinical observations with evoked otoacoustic emissions at Mayo Clinic. *J. Am. Acad. Audiol.*, **14**(4), 213–224.

Smeatham, D. (2002). *Noise Levels and Noise Exposure of Workers in Pubs and Clubs – A Review of the Literature*. HSE books, Norwich NR3 1BQ.

Sokol, J., and M. Hyde (2002). Hearing screening. *Pediat. Rev.*, **23**(5), 155–161.

Stenklev, N.C., and E. Laukli (2003). Transient evoked otoacoustic emissions in the elderly. *Int. J. Audiol.*, **42**(3), 132–139.

Waal, R., R. Hugo, M. Soer and J.J. Kruger (2002). Predicting hearing loss from otoacoustic emissions using an artificial neural network. *S. Afr. J. Commun. Disord.*, **49**, 28–39.

Whitehead, M.L., A.M. Jimenez, B.B. Stagner, M.J. McCoy, B.L. Lonsbury–Martin and G.K. Martin (1995). Time windowing of click evoked otoacoustics emissions to increase signal-to-noise ratio. *Ear Hear*, **16**, 599–611.

A. Janušauskas received the MSc and DSc degrees in electrical and electronics engineering from Kaunas Technology University, Kaunas, Lithuania, in 1996 and 2000, respectively. Since year 2000 he holds a research scientist position at Kaunas Biomedical Engineering Institute. His research interests include biomedical signal processing, detection and time–frequency analysis of otoacoustic emissions, ECG, ICG signal processing, analysis of ultrasonic signals and telemedicine applications.

V. Marozas received his BS in engineering electronics in 1993, MS in metrology and measurements in 1995, and PhD in electrical and electronics engineering from Kaunas University of Technology in 2000. Since year 2000 he has been employed as a research scientist at the Institute of Biomedical Engineering. His research interests include biomedical signal processing, time–frequency analysis, wavelet analysis and neural networks.

A. Lukoševičius received DSc and doctor habilitus degrees in electrical engineering from Kaunas University of Technology (KTU) in 1976 and 1996, respectively. In 1996–2000 he was in position of a vice-rector for research of KTU. Since 2000 he holds a position of professor and director of Biomedical Engineering Institute of KTU. In 2000 he was awarded by National Science Award. His research interests include biomedical engineering, signal and image processing, ultrasound diagnostics, e-health and decision support systems.

L. Sörnmo received the MSc and DSc degrees in electrical engineering from Lund University, Lund, Sweden, in 1978 and 1984, respectively. He held a research position with Department of Clinical Physiology, Lund University, from 1983 to 1995 working with computer-based ECG analysis. Since 1990, he has been at the Signal Processing Group, Department of Electroscience, Lund University, where he now holds a position as a professor in biomedical signal processing. His main research interests include statistical signal processing and modeling of biomedical signals. His current research projects include high-resolution ECG analysis, methods in ischemia monitoring, time–frequency analysis of atrial fibrilation, power efficient signal processing in pacemakers, and detection of otoacoustic emissions. Dr. Sörnmo was on the editorial board of *Computers in Biomedical Research* from 1997 to 2000. Since 2001, he is an associate editor of *IEEE Transactions on Biomedical Engineering*.

Otoakustinės emisijos signalų atpažinimas ir skleidimas laiko ir dažnio plokštumoje Hilberto–Huango trasnformacijos pagalba

Artūras JANUŠAUSKAS, Vaidotas MAROZAS, Arūnas LUKOŠEVIČIUS, Leif SÖRNMO

Straipsnyje pristatyta nauja metodika, skirta impulsu sukeltos otoakustinės emisijos atpažinimui ir skleidimui laikas–dažnis plokštumoje. Metodika pagrįsta pažangia Hilberto–Huango transformacija ir ansamblio koreliacijos metodu. Hilberto–Huango transformacija yra naujas galingas signalų apdorojimo įrankis, skirtas netiesinei nestacionarių signalų analizei, koks yra ir otoakustinės emisijos signalas. Hilberto–Huango transformacija neskiria signalo nuo triukšmo, todėl ši transformacija yra naudojama kartu su ansamblio koreliacijos metodu, signalo intervalų su aukštu signalo ir triukšmo santykiu išskyrimui. Šių metodų kombinacija pateikė labai gerus rezultatus kiek otoakustinės emisijos atpažinimo, tiek ir skleidimo laikas–dažnis plokštumoje prasme. Klinikiniu kriterijumi naudojant 30 dB_{HL} vidutinį klausos slenkstį metodo atpažinimo tikslumas buvo 81% teisingai atpažintų gerai girdinčiųjų signalų, esant 90% neprigirdinčiųjų atpažinimui. Aukšto skiriamumo signalo atvaizdavimas laiko ir dažnio plokštumoje leido nustatyti 70% aukštų dažnių klausos netekimo atvejų. Naudojamas metodas nenaudoja jokios išankstinės informacijos apie signalą ir todėl, padarius minimalius pakeitimus, gali būti taikomas ir kitiems signalams, kuriems naudojamas sinchroninis vidurkinimas.